Int. J. Morphol.,
44(1):291-303, 2026.

Overlapping Distributions of Parvalbumin and Orexin Immunoreactivity in Mouse Brain Regions Associated with Cognitive Function

Distribuciones Superpuestas de la Inmunorreactividad de Parvalbúmina y Orexina en Regiones Cerebrales de Ratón Asociadas con la Función Cognitiva

Haimin Zhang; Jianping Zhang & Maoyun Yuan

ZHANG, H.; ZHANG, J. & YUAN, M. Overlapping distributions of parvalbumin and orexin immunoreactivity in mouse brain regions associated with cognitive function. *Int. J. Morphol., 44(1)*:291-303, 2026.

SUMMARY: Parvalbumin (PV)-positive interneurons play a critical role in modulating cognitive processes. The orexin system is also implicated in the regulation of cognitive function. To provide morphological evidence regarding the neural connection between PV and orexin neurons and their involvement in cognitive function regulation in cognitive function-related brain regions, a double-label immunohistochemical staining for PV and orexin was employed to investigate overlapping distributions of PV and orexin immunoreactivity in these brain regions of the mouse. Somata of PV and orexin neurons were co-localized exclusively in the lateral hypothalamic area (LH), where their fibers were also closely intermingled. In other regions, there were different degrees of contact and overlap between PV neurons and fiber projections of orexin neurons. Within the frontal lobe and temporal lobe, slight-to-moderate density overlap was observed in the orbitofrontal cortex (OFC), medial prefrontal cortex (mPFC), temporal association cortex (TeA) and perirhinal cortex (PRh), while overlap was relatively sparse in the medial entorhinal cortex (MEnt). Low density overlap was detected in the caudate putamen (CPu). Within the basal forebrain (BF), the accumbens nucleus (Acb), medial septal nucleus (MS), nucleus of the vertical limb of the diagonal band (VDB), nucleus of the horizontal limb of the diagonal band (HDB), ventral pallidum (VP), substantia innominata (SI) and magnocellular preoptic nucleus (MCPO) had different degrees of overlap. Slightly overlapping distributions were noted in the field CA1 of hippocampus (CA1) and dentate gyrus (DG) of the hippocampus (HPC). Low density overlap was found in the basolateral amygdaloid nucleus, anterior part (BLA) and central amygdaloid nucleus (Ce) of the amygdala. Within the diencephalon, varying degrees of contact and overlap were observed in the reuniens thalamic nucleus (Re), anterior hypothalamic area (AHA), mediodorsal thalamic nucleus (MD), paraventricular thalamic nucleus (PVT) and zona incerta (ZI). Within the brainstem, in the periaqueductal gray (PAG) and latero-dorsal tegmental nucleus (LDTg), a large number of intermingled orexin fibers and PV branched fine fibers were detected, and overlap was also observed in the ventral tegmental area (VTA). Overall, somata of PV and orexin neurons were co-localized substantially in LH. PV neurons and the fiber projections of orexin neurons were contacted and intermingled to varying degrees in other brain regions implicated in cognitive function regulation. These findings provide morphological evidence supporting a co-regulatory role for the PV and orexin systems in modulating cognitive function.

KEY WORDS: Parvalbumin Orexin; Cognitive function; Memory; Immunohistochemistry.

INTRODUCTION

Cognitive function is a crucial capacity for individuals to receive and process information from the external environment, encompassing various aspects such as attention, executive control, memory, learning, language, and perception. Impairment of cognitive function can lead to severe deficits in learning and memory, social interaction disorders, and other issues, causing patients to lose certain abilities for daily living and social engagement, thereby reducing their quality of life and increasing the burden on families and society (Dolan, 2002). Currently, brain regions known to be associated with cognitive function primarily include the frontal lobe, particularly the orbitofrontal cortex (OFC) (Rudebeck & Rich, 2018) and medial prefrontal cortex (mPFC), several regions within the temporal lobe, such as the temporal association cortex (TeA) (Berger & Ehrsson, 2014), perirhinal cortex (PRh) (Murray *et al*., 2001), and medial entorhinal cortex (MEnt) (Liao *et al*., 2023). Additionally, the caudate putamen (CPu) (Averbeck

Department of Anatomy, Histology and Embryology, School of Basic Medical Sciences, Zhejiang Chinese Medical University, Hangzhou, China.
FUNDING. This work was jointly supported by the second batch of provincial-level teaching reform projects for undergraduate education under the "14th Five-Year Plan" (No. JGBA2024240) and natural science foundation of Zhejiang province (No. ZCLMS25H2901).

Received: 2025-10-13 Accepted: 2026-01-17

et al., 2020) and the basal forebrain (BF) are also involved in cognitive function, with the BF encompassing regions such as the accumbens nucleus (Acb), medial septal nucleus (MS), nucleus of the vertical limb of the diagonal band (VDB), nucleus of the horizontal limb of the diagonal band (HDB), ventral pallidum (VP), substantia innominata (SI), and magnocellular preoptic nucleus (MCPO). Other critical regions include the hippocampus (HPC), the amygdala (Averbeck *et al*., 2020), and certain regions within the diencephalon, such as the reuniens thalamic nucleus (Re), anterior hypothalamic area (AHA) (Roy *et al*., 2022), mediodorsal thalamic nucleus (MD) (Averbeck *et al*., 2020), paraventricular thalamic nucleus (PVT), zona incerta (ZI) (Zhou *et al*., 2018), and lateral hypothalamic area (LH) (Liao *et al*., 2023). Furthermore, several areas within the midbrain, including the ventral tegmental area (VTA) (La Barbera *et al*., 2022), periaqueductal gray (PAG), and laterodorsal tegmental nucleus (LDTg) (Roy *et al*., 2022), as well as the cerebellum (Carta *et al*., 2019), are also implicated.

Orexin is an excitatory neuropeptide encoded by a specific mRNA in hypothalamic orexin neurons and exists in two isoforms, orexin-A (OXA) and orexin-B (OXB) (Peyron *et al*., 1998). Orexin neurons are specifically localized in the perifornical area, lateral hypothalamus, dorsomedial hypothalamus, and posterior hypothalamus, and they extensively project throughout the brain, innervating multiple brain regions closely associated with cognition (Nambu *et al*., 1999). Since its discovery in 1998, orexin has been extensively studied and confirmed to be involved in regulating various neurophysiological functions. Recent reports have increasingly demonstrated its role in modulating cognitive processes. Studies disrupting local or systemic orexin signaling have revealed that orexin plays a role in the regulation of attention, cognitive function, and stress-induced attenuation of cognitive flexibility (Durairaja & Fendt, 2021). Furthermore, recent study indicated a role for orexin in rodent cognition and attention, with supporting evidence coming from impairments in executive control and working memory observed in human narcolepsy patients lacking orexin neurons (Bayard *et al*., 2012). Additionally, orexin is also believed to be associated with neuropsychiatric disorders characterized by cognitive deficits, such as schizophrenia (Deutch *et al*., 2007), attention deficit hyperactivity disorder (ADHD) (Cortese *et al*., 2008), and neurodegenerative diseases like Alzheimer's disease (Fronczek *et al*., 2012; Chen *et al*., 2015).

Parvalbumin (PV) is an intracellular calcium-binding protein belonging to the elongated factor hand domain superfamily of calcium-regulatory proteins, primarily functioning as an intracellular Ca^{2+} buffer (Hontanilla *et al*., 1998). PV-positive interneurons (PV-INs), a major subtype of GABAergic inhibitory interneurons associated with regulatory inhibition (McKenna *et al*., 2013), are widely distributed throughout the brain, including multiple regions implicated in cognition. Substantial evidence has established the critical role of PV-INs in regulating cognitive function. PV-INs are essential formaintaining the dynamic balance between excitation and inhibition (E/I balance) within neural networks and contribute to the generation of gamma neural oscillations (Buzsáki & Wang, 2012), thereby influencing neuronal encoding, information processing, and transmission, and playing a key role in cognitive processes such as learning and memory, attention, arousal states, and social interaction. It has been reported that the loss of PV-INs contributed to sensory deficits (Chen *et al*., 2018) and impaired memory function (Roque *et al*., 2023). Furthermore, studies have shown that PV-INs are associated with neuropsychiatric disorders characterized by cognitive deficits, such as schizophrenia (Pantazopoulos *et al*., 2007), epilepsy (Franz *et al*., 2023), and Alzheimer's disease (Lewis *et al*., 2022).

In this study, we employed immunohistochemical staining to map the distributions and examine the overlap of PV and orexin neurons, along with their fiber projections, within the aforementioned cognitive-related brain regions or nuclei in mice. These findings provide morphological evidence supporting the potential collaborative role of the PV and orexin systems in modulating cognitive function within these brain regions.

MATERIAL AND METHOD

Experimental Animals. Male SPF inbred C57BL/6J mice (Shanghai SLAC Laboratory Animal Co., Ltd., China), each weighing about 22-25 g, were housed in the Laboratory Animal Research Centre of Zhejiang Chinese Medical University. Animals were acclimatized in a controlled environment with a 12/12-hour light/dark cycle (lights on at 07:00 and off at 19:00), an ambient temperature of 20 - 25°C, and 55 - 60 % relative humidity, with ad libitum access to standard diet and water. All experimental procedures were designed to minimize animal discomfort and the number of animals used.

Ethical consideration. All experimental procedures involving animals were approved and performed in strict adherence to the animal guidelines established by the Laboratory Animal Research Centre of Zhejiang Chinese Medical University, Hangzhou, in Zhejiang province. (Protocol Number: IACUC-20220627-07).

Tissue preparation. Following deep anesthesia with sodium pentobarbital (60 mg/kg, i.p.) and verification of areflexia (mice were unresponsive to tail- or foot-pinching), mice (n=4) underwent transcardial perfusion with saline followed by 4 % paraformaldehyde at room temperature. The isolated brains were then post-fixed in 4 % paraformaldehyde for 4 h at 4 °C. Following fixation, the tissues were subjected to dehydration through the graded sucrose solutions (10 %, 20 % and 30 %) at 4 ˚C until sinking. Coronal sections (30 μm) were prepared using a Leica freezing microtome (Leica, type 820-II), collected into four sets, and stored at -20°C in cryoprotectant until staining.

Immunohistochemical procedures. The first set of free-floating sections was rinsed in phosphate-buffered saline (PBS) and then treated with 3 % H_2O_2 in PBS for 30 min. After rinsing, the sections were blocked for 1 h at room temperature with a solution containing 10 % goat serum (Cat. No. S-1000, Vector Laboratories, Tucson, AZ, USA) and 0.3 % Triton X-100 in PBS. Removing the solution without washing, the sections were incubated overnight at 4 °C with the primary antibodies, which consisted of a monoclonal mouse anti-orexin antibody (1:1,000; Cat. No. sc-80263, Santa Cruz Biotechnology, Santa Cruz, CA, USA) to identify orexin neurons and a monoclonal rabbit anti-PV antibody (1:1,000; Cat. No. ab181086, Abcam, Cambridge, UK) to identify PV neurons. Following primary incubation, the sections were rinsed and subsequently incubated for 2 h at room temperature with secondary antibodies, comprising a biotinylated goat anti-mouse IgG antibody (Cat. No. BA-9200, Vector Laboratories, Burlingame, CA, USA) and a biotinylated goat anti-rabbit IgG antibody (Cat. No. BA-1000, Vector Laboratories), followed by avidin-biotin-horseradish peroxidase complex (ABC) solution (Vectastain Elite ABC Kit; Vector Laboratories; Cat. No. PK-4000). The sections were rinsed with PBS and then visualized with diaminobenzidine (DAB) in the presence of nickel ammonium sulphate. Finally, the stained sections were rinsed, mounted on gelatin-coated slides, air-dried overnight, dehydrated through a graded ethanol series, cleared in xylene, and coverslipped.

Microscopy. An Olympus IX71 microscope was used for image acquisition. The anatomical landmarks employed in this study were based on a mouse brain atlas. The outlines of the sections and major structures were evaluated at low magnification (4x), followed by mapping the profiles of the immunoreactive neurons using high magnification. All digital photomicrographs were processed with Adobe Photoshop CS2.

RESULTS

Frontal lobe. In the frontal lobe, we primarily examined the overlapping distributions of PV neurons and orexin fibers in the OFC and mPFC. The OFC can be broadly subdivided into the medial orbital cortex (MO), ventral orbital cortex (VO), lateral orbital cortex (LO), dorsolateral orbital cortex (DLO), and agranular insular cortex (AI). Notable overlap between PV neurons and orexin fibers was observed in the first three subregions (MO, VO, LO). Medium-to-high densities of PV neurons were distributed in the VO (Fig. 1A, 1C) and LO (Fig. 1A, 1D), while their distributions in the MO (Fig. 1A, 1B) were relatively sparse. Axons and branched dendrites of PV neurons were readily observable, often exhibiting terminal boutons. Orexin fibers, characterized by their slender, varicose morphology and terminal boutons, exhibited a similar density across these three OFC subregions, intermingling with PV neurons and demonstrating contact or overlap with them. The mPFC mainly consists of three subregions: thecingulate cortex area 1 (Cg1) (Fig. 1E, 1F), prelimbic cortex (PrL) (Fig. 1E, 1G), and infralimbic cortex (IL) (Fig. 1E, 1H). The pattern of overlap between PV neurons and orexin fibers was similar across these subregions. Medium-sized PV neuronal somata and their processes were distributed at a moderate density throughout the mPFC. Thin, varicose orexin fibers and their boutons were randomly dispersed across these regions, frequently contacting or overlapping with PV neurons.

Temporal lobe. Within the three examined temporal regions, overlapping distributions of PV and orexin immunoreactivity were observed in the TeA (Fig. 5E, 5F) and PRh (Fig. 5E, 5G). These areas contained a moderate density of PV neuronal somata and their fine processes, intermingled with slender, varicose orexin fibers and their boutons. Close contacts and overlaps between the two were readily observable. In contrast, the overlap within the MEnt (Fig. 6E, 6F) was relatively sparse.

Caudate putamen (CPu). Within the CPu, both PV neurons and orexin fibers were sparsely distributed. Orexin fibers appeared short, thin, and curved, with few terminal boutons, while PV neurons exhibited several fine dendritic branches. Despite the sparse distribution, interweaving and overlapping between the two types of fibers could still be observed (Fig. 2A, 2B).

Basal forebrain (BF). In the BF, overlapping distributions were primarily observed in the following regions: In the Acb (Fig. 2C, 2D) and SI (Fig. 3C, 3D), only fibers from both neuron types were observed,

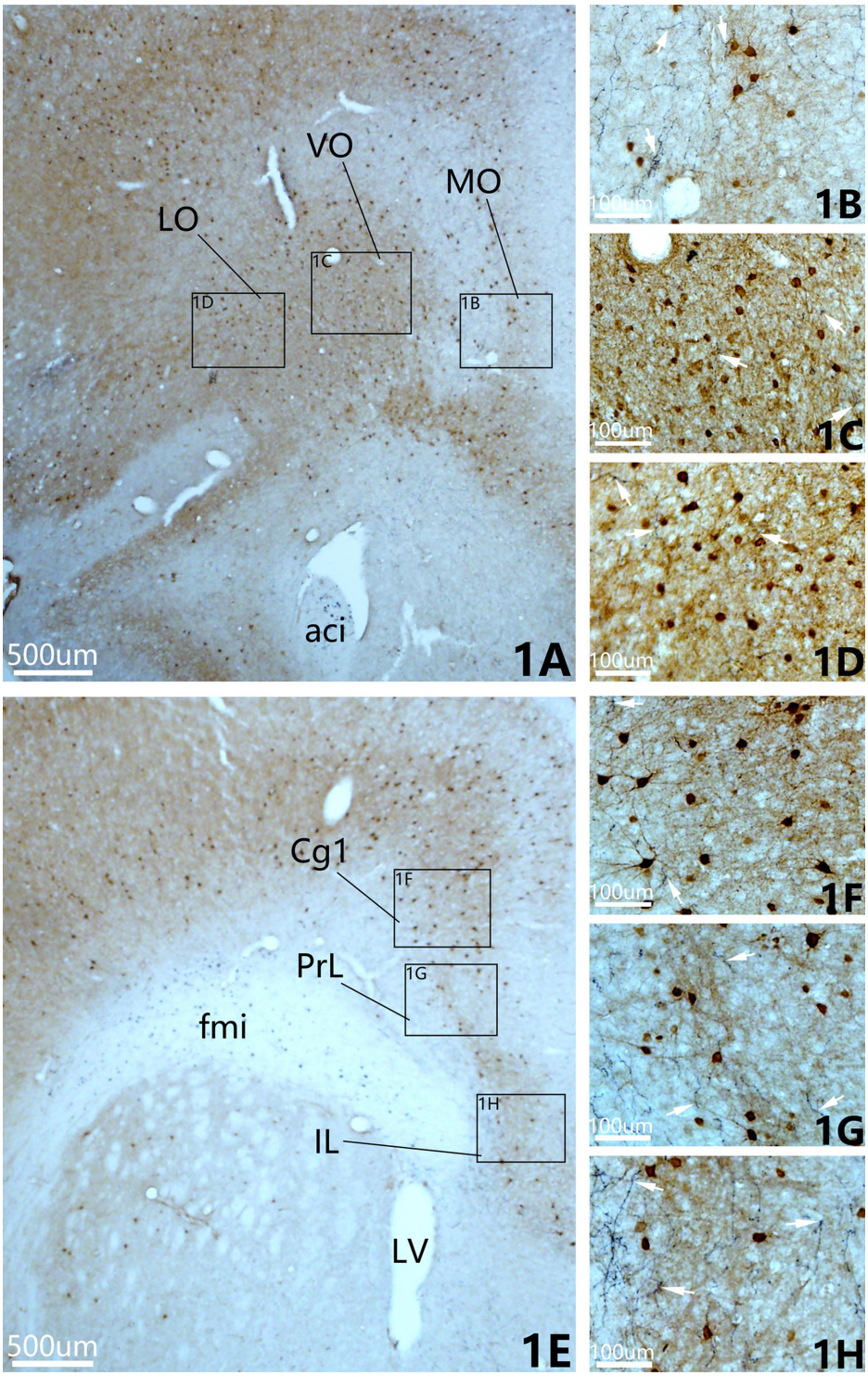

Fig. 1. Brightfield images depicting intermingled PV and orexin immunoreactivity in the medial orbital cortex (MO, 1A, 1B), ventral orbital cortex (VO, 1A, 1C), lateral orbital cortex (LO, 1A, 1D), the cingulate cortex area 1 (Cg1) (Fig. 1E, 1F), prelimbic cortex (PrL) (Fig. 1E, 1G), and infralimbic cortex (IL) (Fig. 1E, 1H). 1B-1D, 1F-1H are higher-magnification images of the boxed areas depicted in the two photomicrographs in the left column. PV immunoreactive elements stained with monoclonal rabbit anti-PV, appear brown; orexin immunopositive elements stained with monoclonal mouse anti-orexin, appear black. Abbreviations: aci, anterior commissure, intrabulbar part; fmi, forceps minor of the corpus callosum; LV, lateral ventricle. Scale bars=500 µm at the bottom of photomicrograph in 1A, 1E, 100 µm in 1B-1D, 1F-1H.

predominantly thin, elongated, and curved, interwoven with one another. Orexin fibers in the Acb displayed larger boutons, some of which were embedded within PV fibers. In the MS (Fig. 2E, 2F), VDB (Fig. 2G, 2H), HDB (Fig. 2G, 2I), VP (Fig. 3A, 3B), and MCPO (Fig. 3E, 3F), large PV neuronal somata and thick, long fibers were readily observed. These PV neurons displayed prominent axons and dense dendritic branching. Within these regions, thin, elongated, and varicose orexin fibers with large boutons were intermingled with the PV elements, showing extensive contacts and overlaps.

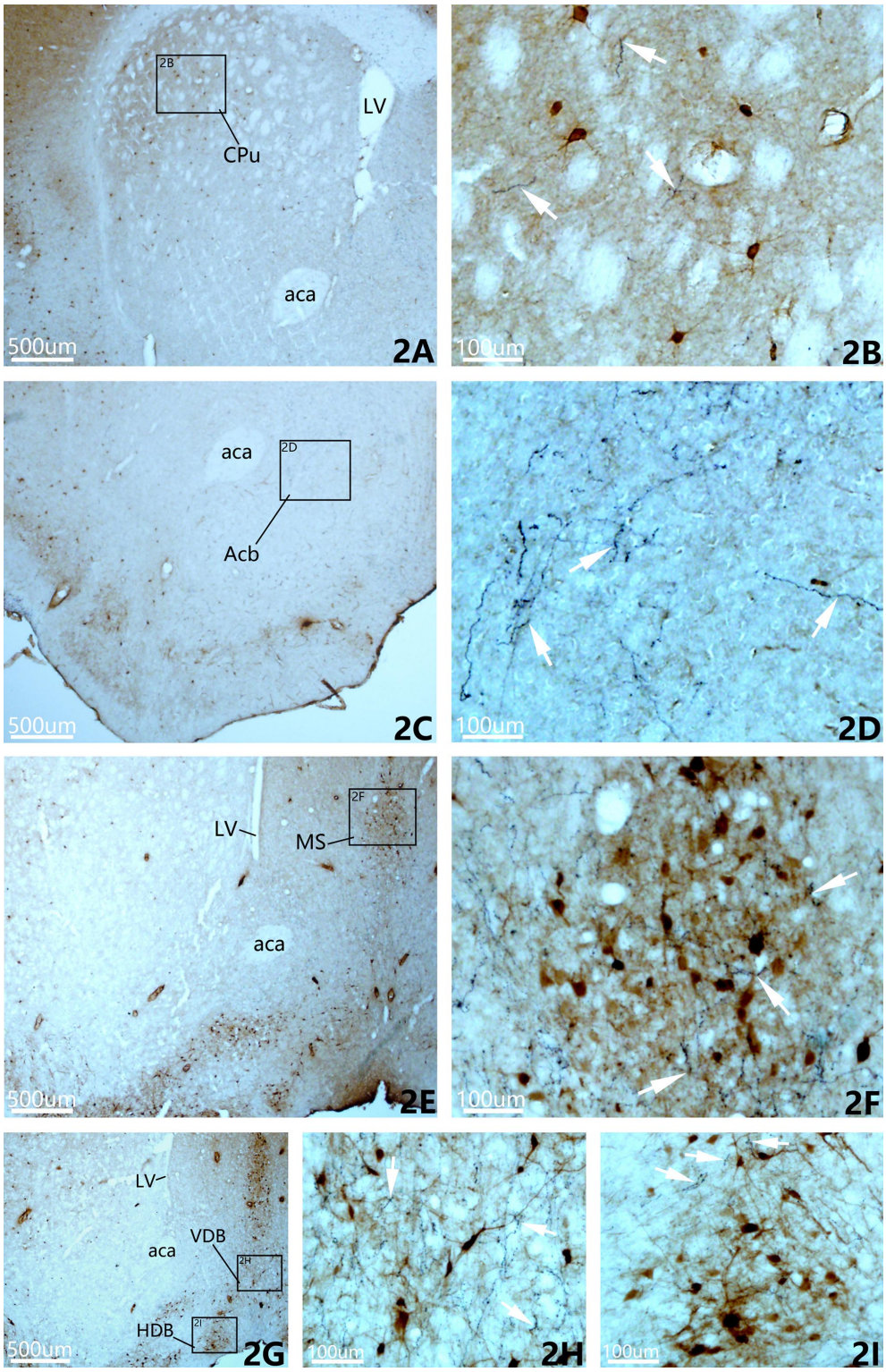

Fig. 2. Brightfield images depicting intermingled PV and orexin immunoreactivity in the caudate putamen (CPu, 2A, 2B), accumbens nucleus (Acb, 2C, 2D), medial septal nucleus (MS, 2E, 2F), nucleus of the vertical limb of the diagonal band (VDB, 2G, 2H), and nucleus of the horizontal limb of the diagonal band (HDB, 2G, 2I). 2B, 2D, 2F, 2H, 2F are higher-magnification images of the boxed areas depicted in the four photomicrographs in the left column. PV immunoreactive elements stained with monoclonal rabbit anti-PV, appear brown; orexin immunopositive elements stained with monoclonal mouse anti-orexin, appear black. Abbreviations: aca, anterior commissure, anterior part; LV, lateral ventricle. Scale bars=500 μm at the bottom of photomicrograph in 2A, 2C, 2E, 2G, 100 μm at the bottom of photomicrograph in 2B, 2D, 2F, 2H, 2I.

Hippocampus (HPC). In the HPC, sparse overlap was observed in the field CA1 of hippocampus (CA1) (Fig. 4D, 4E) and dentate gyrus (DG) (Fig. 4D, 4F). These regions contained a low density of short, thin, and curved orexin fibers. PV immunoreactivity was also scarce, with only a few neuronal somata and short, fine processes present in the HPC. Some orexin boutons were embedded within PV fibers.

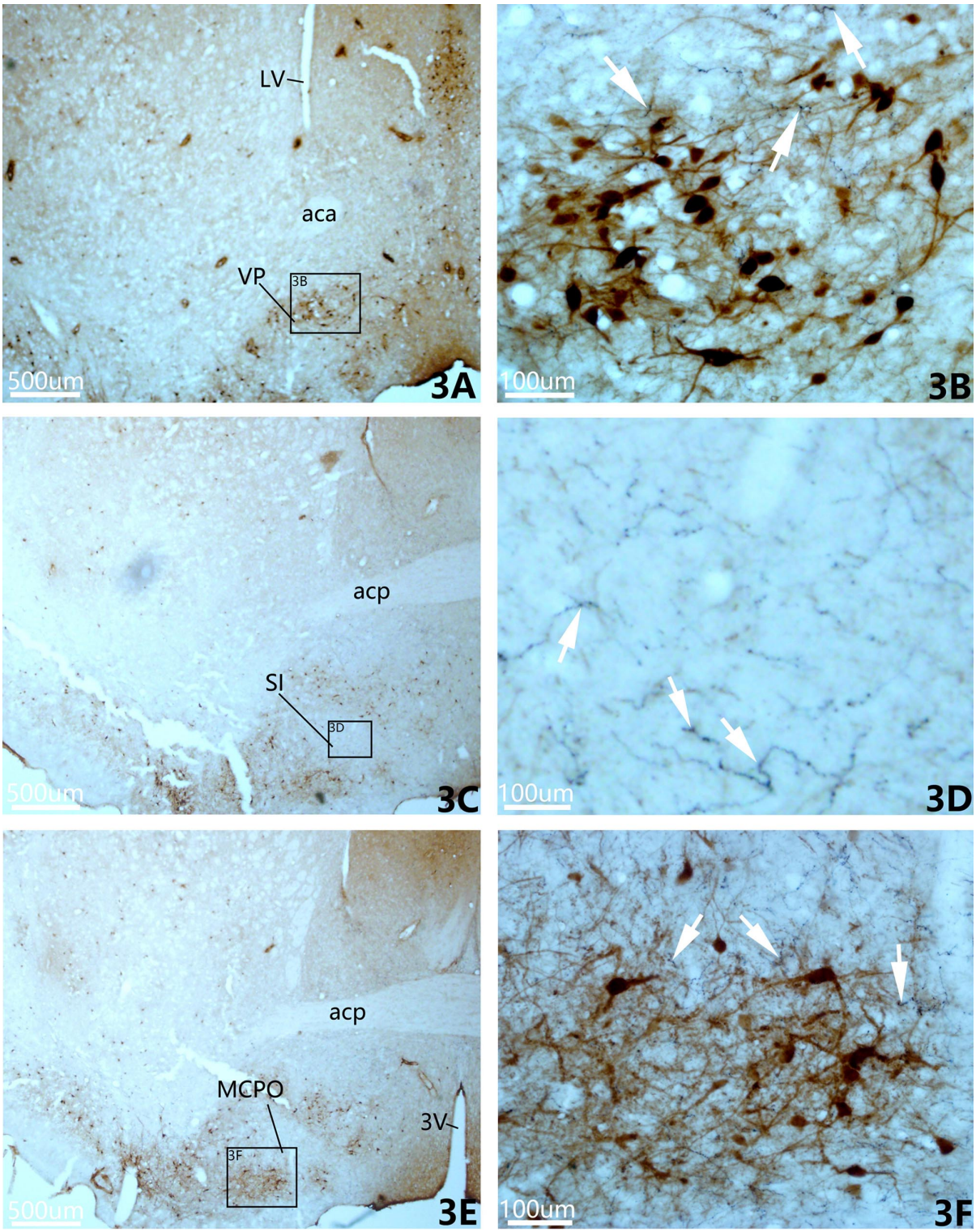

Fig. 3. Brightfield images depicting intermingled PV and orexin immunoreactivity in the ventral pallidum (VP, 3A, 3B), substantia innominata (SI, 3C, 3D), and magnocellular preoptic nucleus (MCPO, 3E, 3F). 3B, 3D, 3F are higher-magnification images of the boxed areas depicted in the three photomicrographs in the left column. PV immunoreactive elements stained with monoclonal rabbit anti-PV, appear brown; orexin immunopositive elements stained with monoclonal mouse anti-orexin, appear black. Abbreviations: LV, lateral ventricle; aca, anterior commissure, anterior part; acp: anterior commissure, posterior; 3V, 3rd ventricle. Scale bars=500 μm at the bottom of photomicrograph in 3A, 3C, 3E, 100 μm in 3B, 3D, 3F.

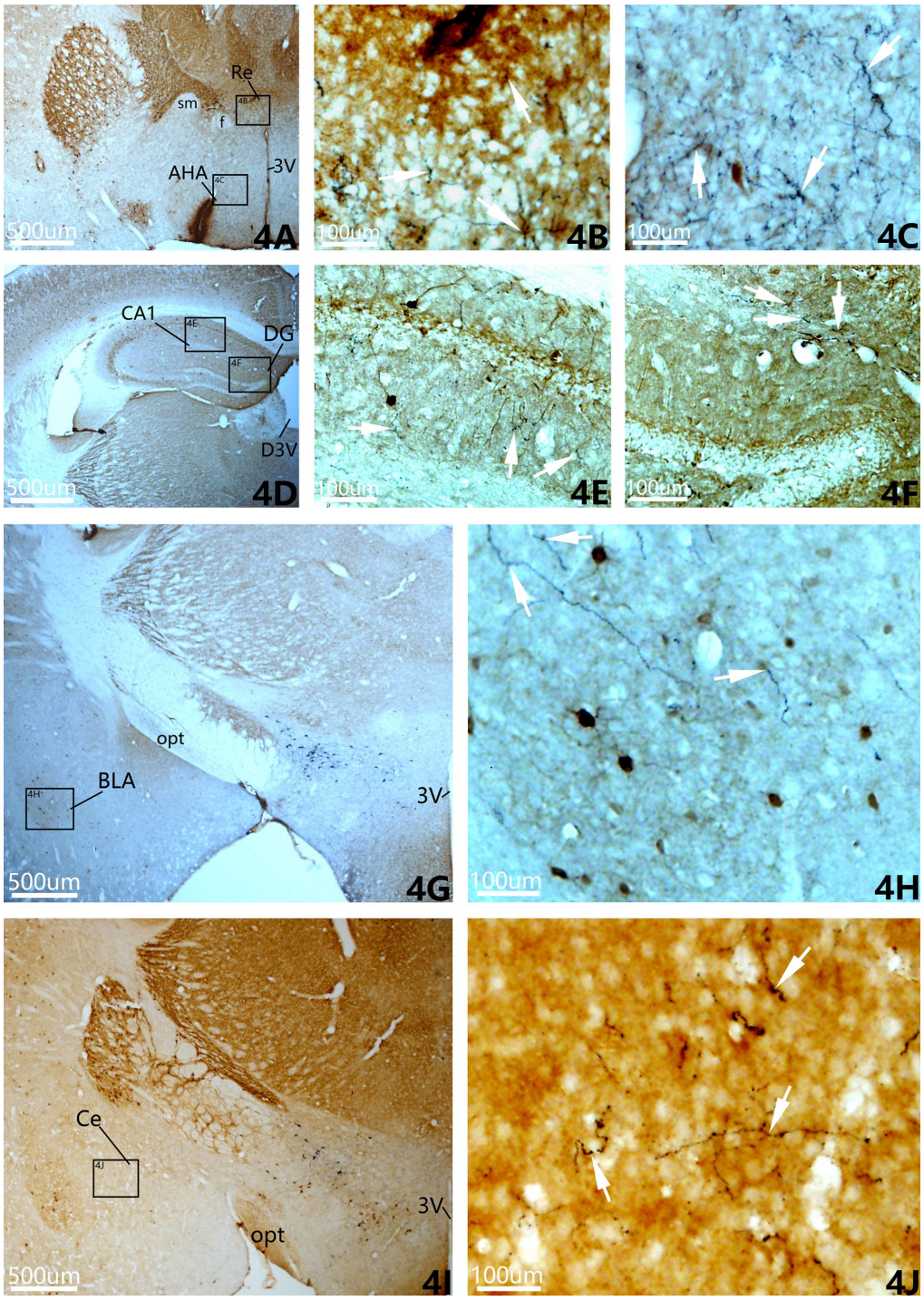

Fig. 4. Brightfield images depicting intermingled PV and orexin immunoreactivity in the reuniens thalamic nucleus (Re, 4A, 4B), anterior hypothalamic area (AHA, 4A, 4C), field CA1 of hippocampus (CA1, 4D, 4E) and dentate gyrus (DG, 4D, 4F), basolateral amygdaloid nucleus, anterior part (BLA, 4G, 4H) and central amygdaloid nucleus (Ce, 4I, 4J). 4B, 4C, 4E, 4F, 4H, 4J are higher-magnification images of the boxed areas depicted in the four photomicrographs in the left column. PV immunoreactive elements stained with monoclonal rabbit anti-PV, appear brown; orexin immunopositive elements stained with monoclonal mouse anti-orexin, appear black. Abbreviations: sm, stria medullaris of the thalamus; f, fornix; 3V, 3rd ventricle; D3V, dorsal 3rd ventricle; opt, optic tract. Scale bars=500 μm at the bottom of photomicrograph in 4A, 4D, 4G, 4I, 100 μm in 4B, 4C, 4E, 4F, 4H, 4J.

Amygdala. Within the anterior part of the basolateral amygdaloid nucleus (BLA), a moderate density of PV neuronal somata and fibers was observed. The PV fibers contained few and thin axons, with mostly branched, fine dendrites. Thin, elongated, and varicose orexin fibers were intermingled among them, and contacts and overlaps between the two could be observed (Fig. 4G, 4H). In the central amygdaloid nucleus (Ce), only PV fibers and orexin fibers with relatively large boutons were visible, both at low density. Fine PV fibers and varicose orexin fibers were randomly dispersed and in contact with each other. Some orexin boutons were embedded within PV fibers (Fig. 4I, 4J).

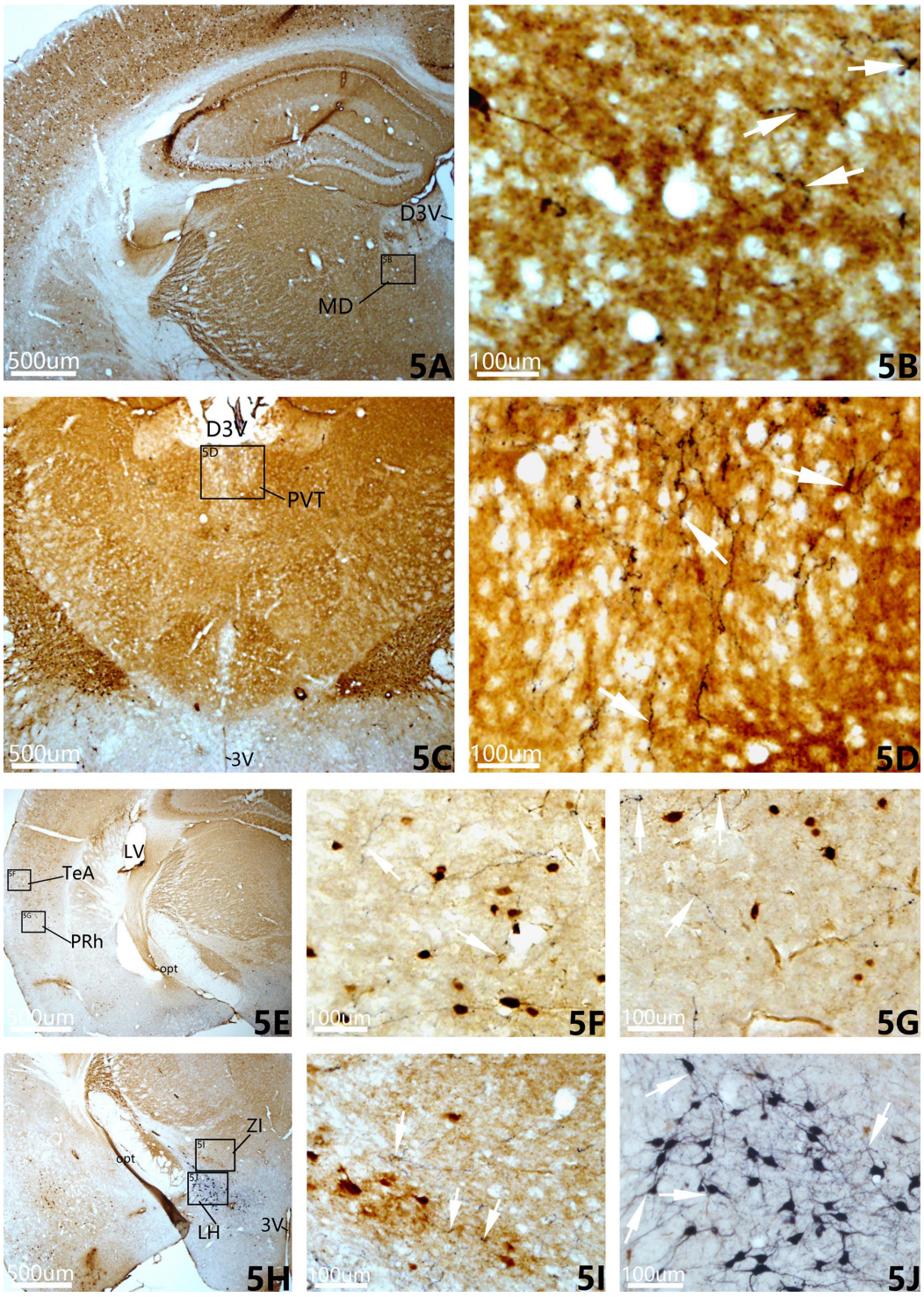

Fig. 5. Brightfield images depicting intermingled PV and orexin immunoreactivity in the mediodorsal thalamic nucleus (MD, 5A, 5B), paraventricular thalamic nucleus (PVT, 5C, 5D), temporal association cortex (TeA, 5E, 5F), perirhinal cortex (PRh, 5E, 5G), zona incerta (ZI, 5H, 5I), and lateral hypothalamic area (LH, 5H, 5J). 5B, 5D, 5F, 5G, 5I, 5J are higher-magnification images of the boxed areas depicted in the four photomicrographs in the left column. PV immunoreactive elements stained with monoclonal rabbit anti-PV, appear brown; orexin immunopositive elements stained with monoclonal mouse anti-orexin, appear black. Abbreviations: D3V, dorsal 3rd ventricle; 3V, 3rd ventricle; LV, lateral ventricle; opt, optic tract. Scale bars=500 μm at the bottom of photomicrograph in 5A, 5C, 5E, 5H, 100 μm in 5B, 5D, 5F, 5G, 5I, 5J.

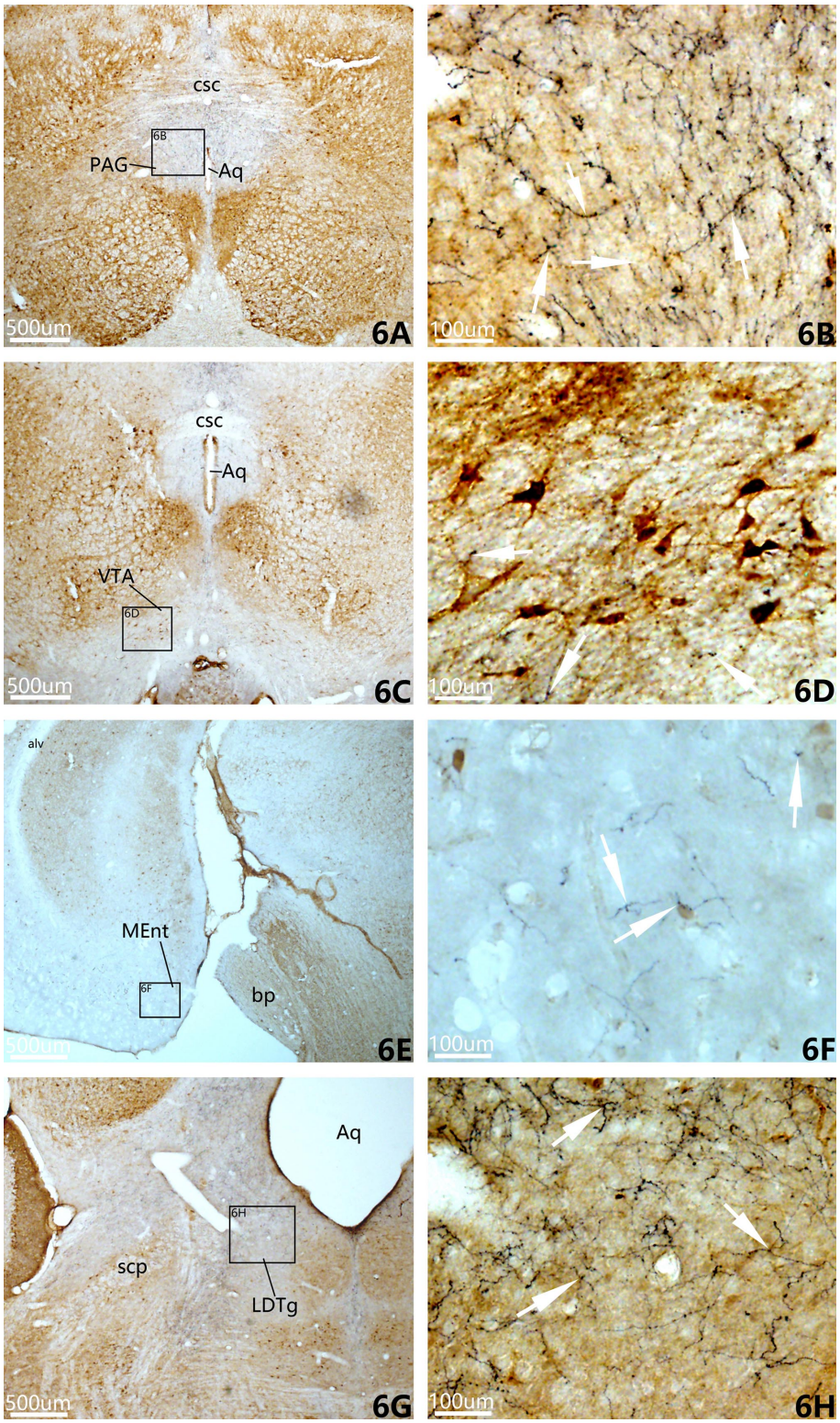

Fig. 6. Brightfield images depicting intermingled PV and orexin immunoreactivity in the periaqueductal gray (PAG, 6A, 6B), the ventral tegmental area (VTA, 6C, 6D), medial entorhinal cortex (MEnt, 6E, 6F), and laterodorsal tegmental nucleus (LDTg, 6G, 6H). 6B, 6D, 6F, 6H are higher-magnification images of the boxed areas depicted in the four photomicrographs in the left column. PV immunoreactive elements stained with monoclonal rabbit anti-PV, appear brown; orexin immunopositive elements stained with monoclonal mouse anti-orexin, appear black. Abbreviations: csc, commissure of the superior colliculus; Aq, aqueduct; bp, brachium pontis (stem of middle cerebellar peduncle); scp, superior cerebellar peduncle (brachium conjunctivum). Scale bars=500 µm at the bottom of photomicrograph in 6A, 6C, 6E, 6G, 100 µm in 6B, 6D, 6F, 6H.

Diencephalon. In the Re (Fig. 4A, 4B), MD (Fig. 5A, 5B), and PVT (Fig. 5C, 5D), numerous orexin fibers with varicosities and large boutons were observed. These fibers were randomly dispersed among moderately dense, elongated, and branched PV fibers. Close contacts and overlaps between the two fiber types were frequently noted, with many orexin boutons embedded within PV fibers. Within the AHA, only very few PV neuronal somata were

observed. However, both branched PV fibers and thin, elongated, varicose orexin fibers were densely distributed in this region. The two types of fibers were extensively intermingled, with numerous orexin boutons embedded within PV fibers (Fig. 4A, 4C). In the ZI, low-to-moderate densities of PV neuronal somata and fibers were present. Short, curved orexin fibers were randomly dispersed among them, showing contacts and overlaps with PV elements (Fig. 5H, 5I). Notably, somata of both PV and orexin neurons were exclusively co-localized in the LH. In this region, both PV and orexin neurons were densely distributed, with their somata, thick axons, and fine, branched dendrites clearly observable. Their somata were in close contact and highly overlapping. Their fibers were extensively interwoven (Fig. 5H, 5J).

Brainstem. In the PAG (Fig. 6A, 6B) and LDTg (Fig. 6G, 6H), a substantial number of orexin fibers exhibiting varicosities and numerous boutons were observed intermingling with moderately to highly dense, finely branched PV fibers. A considerable number of orexin boutons were embedded within PV fibers. Within the VTA, moderately dense, relatively large PV neuronal somata and elongated fibers were present, with their axons clearly identifiable. In contrast, only sparse, thin orexin fibers with their boutons were observed in this region. Contacts and overlaps between orexin fibers and PV elements were relatively limited in the VTA (Fig. 6C, 6D).

DISCUSSION

In this study, we employed immunohistochemical DAB staining to morphologically characterize the distributions and overlap between PV neurons and orexin neurons, along with their fiber projections, across cognitive-related brain regions in mice. Although orexin neurons are relatively sparse and specifically localized to the perifornical area, lateral hypothalamus, dorsomedial hypothalamus, and posterior hypothalamus, they project extensively throughout the brain. Previous work delineated the distributions of orexin neurons and their projections across the rat brain, including the cognitive-related regions examined in our study (Peyron *et al*., 1998; Nambu *et al*., 1999). Earlier research in rats has shown that PV is expressed in a subpopulation of large GABAergic neurons that project to the cortex (Gritti *et al*., 2003). Subsequently, researchers described the distributions of PV neurons within various nuclei of the rat basal ganglia (Hontanilla *et al*., 1998) and mouse BF (McKenna *et al*., 2013), respectively. In the basal ganglia, PV neurons were primarily located in regions such as the CPu and globus pallidus (GP) (Hontanilla *et al*., 1998). Within the BF, PV neuron density was highest in the MCPO, followed by the VP and the HDB, with the SI showing the lowest density. PV neurons exhibited medium to large somata and were less abundant in the rostral BF compared to the medial and caudal BF (McKenna *et al*., 2013). Furthermore, Celio *et al*. (2013) observed isolated clusters of PV-positive neurons in the rodent LH, featuring small to medium-sized somata that were more numerous rostrally than caudally, and intermingled with thick axons of the medial forebrain bundle (Mészár *et al*., 2012). The distribution patterns of PV and orexin immunoreactivity observed in the present study across the aforementioned cognitive-related brain regions were consistent with these previously reported findings, thereby validating the scientific reliability of our experimental results.

Through immunohistochemical DAB staining, we observed overlapping distributions of PV and orexin immunoreactivity in the following cognitive-related brain regions in mice (Figs. 1 to 6): Somatic co-localization of PV and orexin neurons, accompanied by interwoven fibers, were exclusively detected in the LH. In all other regions, varying degrees of contact and overlap were observed between PV elements and orexin projection fibers. Moderate overlap was noted in the OFC and mPFC of the frontal lobe, as well as in the TeA, PRh, and MEnt of the temporal lobe. Within the BF, varying degrees of overlap were observed primarily in the Acb, MS, VDB, HDB, VP, SI, and MCPO. Sparse overlap was seen in the CPu, the CA1 and DG of the HPC, as well as the BLA and Ce of the amygdala. In the diencephalon, different degrees of contact and overlap were observed in the Re, AHA, MD, PVT, and ZI. In the brainstem, extensive intermingling of orexin fibers and finely branched PV fibers were found in the PAG and LDTg, with overlap also present in the VTA.

The MEnt is a key structure for learning and memory, primarily responsible for the encoding, consolidation, storage, and retrieval of spatially relevant information, playing a vital role in cognitive processes such as spatial learning and memory (Sasaki *et al*., 2015). Neurons within the MEnt include excitatory principal projection neurons and inhibitory interneurons, among which PV-INs represent a major inhibitory subtype (Martínez *et al*., 2017). An important electrophysiological signature of spatial information processing in the MEnt is the presence of gamma and theta oscillations in the local field potential (Nakazono *et al*., 2018). The activity of interneurons, particularly PV-positive neurons, and the inhibitory postsynaptic currents (IPSCs) they generate are generally considered to form the electrophysiological basis of gamma oscillations (Buzsáki & Wang, 2012). Reduced density of PV-INs has been observed in the MEnt of individuals with schizophrenia and relevant animal models

(Pantazopoulos *et al*., 2007), further supporting the functional importance of PV-INs in higher cognitive processes. Studies have shown that orexin neurons in the LH exhibit high levels of activation during spatial memory-related behaviors, and retrograde neural tracing has confirmed that these neurons project to the MEnt (Liao *et al*., 2023). Furthermore, chemogenetic inhibition of the orexin - MEnt pathway impaired spatial memory, whereas optogenetic activation of this pathway enhanced it (Liao *et al*., 2023), suggesting a role for orexin projections to the MEnt in spatial memory. In the present study, we also observed overlapping distributions of PV elements and orexin projections within the MEnt (Fig. 6E, 6F). Based on this collective evidence, we propose the following hypothesis: Orexin neurons in the LH send projections to the MEnt, where they release orexin to excite principal projection neurons. These excited principal projection neurons, in turn, activate local interneurons, including PV-INs, leading to generated IPSCs and increased gamma oscillatory activity, through which strengthen spatial information processing in the MEnt, thereby improving spatial learning and memory. These findings suggested that the PV and orexin systems act in concert within the MEnt to support normal cognitive function.

The HPC plays a central role in memory and learning, with one of its most well-established functions being the formation of a cognitive map of space, making it essential for spatial learning and memory. Orexin can directly project to the HPC to influence learning and memory. For instance, intra-hippocampal administration of OXA has been reported to ameliorate early-dependent memory impairment in a mouse model of social cognitive dysfunction associated with Parkinson's disease (Stanojlovic *et al*., 2019). Additionally, upregulating the activity of PV-INs in the HPC has been shown to enhance gamma oscillations and significantly reverse pathological alterations in animal models of cognitive impairment (Iaccarino *et al*., 2016). Elevated orexin concentration in the cerebrospinal fluid has been observed in patients with behavioral variant frontotemporal dementia, suggesting that orexin in the frontal and temporal lobes can influence cognition (Roveta *et al*., 2022). Studies in a mouse model of epilepsy revealed a reduction in the number of PV-INs in the temporal lobe, leading to diminished inhibition on granule cells, thereby causing cortical hyperexcitability and seizures, as well as significant cognitive deficits (Franz *et al*., 2023). Furthermore, the orexin system has been shown to modulate cognitive responses to potential threat stimuli via both OXA and OXB receptors in the mPFC (Soares *et al*., 2021). The therapeutic agent of Alzheimer's disease memantine has demonstrated the ability to improve cognitive dysfunction by modulating E/I balance in the mPFC through actions on PV-INs (Lewis *et al*., 2022). In the present study, we observed overlapping distributions of PV elements and orexin projection fibers in the CA1 (Fig. 4D, 4E) and DG (Fig. 4D, 4F) of the HPC, the TeA (Fig. 5E, 5F) and PRh (Fig. 5E, 6G) of the temporal lobe, and the mPFC (Fig. 1E-H). Collectively, this evidence suggested that the PV and orexin systems act in concert within these brain regions to co-regulate cognitive processes, thereby contributing to normal cognitive function.

As previously mentioned, orexin neurons in the LH exhibited high levels of activation during spatial memory-related behaviors, suggesting their involvement in spatial memory processes (Liao *et al*., 2023). Furthermore, activation of the orexin - BF pathway was known to enhance acetylcholine release and increase the activity of cortical neurons, thereby supporting attentional processing during wakefulness and contributing to the cognitive components of motivated behavior. Although there are relatively few reports directly addressing the role of PV in regulating cognitive function specifically within the LH (Fig. 5H, 5J) and the constituent nuclei of the BF, including the Acb (Fig. 2C, 2D), MS (Fig. 2E, 2F), VDB (Fig. 2G, 2H), HDB (Fig. 2G, 2I), VP (Fig. 3A, 3B), SI (Fig. 3C, 3D), and MCPO (Fig. 3E, 3F), the overlapping distributions of PV and orexin immunoreactivity observed in these nuclei in the present study suggested that a cooperative role between the PV and orexin systems in the modulation of cognition within these regions cannot be excluded.

In the present study, overlapping distributions of PV elements and orexin projection fibers were also observed in the OFC (Fig. 1A-D), CPu (Fig. 2A, 2B), Re (Fig. 4A, 4B), AHA (Fig. 4A, 4C), BLA (Fig. 4G, 4H), Ce (Fig. 4I, 4J), MD (Fig. 5A, 5B), PVT (Fig. 5C, 5D), ZI (Fig. 5H, 5I), PAG (Fig. 6A, 6B), VTA (Fig. 6C, 6D), and LDTg (Fig. 6G, 6H). Although the regulatory roles of the PV and orexin systems within these specific regions in cognition have rarely been reported, our morphological findings provide an anatomical foundation for future related investigations.

The PV and orexin systems are co-localized across multiple brain regions involved in cognitive function, where they exhibit close contacts and extensive intermingling, with their distributions precisely respecting identical boundaries in several areas. Although methodological variations and antibody specificities may influence staining sensitivity and intensity, our results consistently demonstrated numerous instances of clear contacts and overlaps between PV elements and orexin fibers, including their boutons. This morphological

evidence suggested potential synaptic interactions and functional cooperation between these two systems. Maintaining dynamic E/I balance within neural circuits and networks is fundamental for normal electrophysiological activity and higher cognitive function. PV-INs play a pivotal role in regulating this E/I balance, while orexin neurons are known to exert modulatory effects on relevant GABAergic systems. The observed anatomical convergence may thus represent a structural basis for their coordinated regulation of cognitive processes.

CONCLUSIONS

In summary, somata of PV and orexin neurons are co-localized and exhibit marked overlap within the LH. Furthermore, PV elements and orexin fiber projections demonstrated varying degrees of intermingling and overlap across multiple other brain regions implicated in cognitive regulation, including the frontal and temporal cortices, HPC, and other key areas governing cognitive processes. This study provides morphological evidence supporting a cooperative role for the PV and orexin systems in the maintenance of normal cognitive function.

ACKNOWLEDGMENTS

This work was jointly supported by the second batch of provincial-level teaching reform projects for undergraduate education under the "14th Five-Year Plan" (No. JGBA2024240) and natural science foundation of Zhejiang province (No. ZCLMS25H2901).

ZHANG, H.; ZHANG, J. & YUAN, M. Distribuciones superpuestas de la inmunorreactividad de parvalbúmina y orexina en regiones cerebrales de ratón asociadas con la función cognitiva. *Int. J. Morphol., 44(1)*:291-303, 2026.

RESUMEN: Las interneuronas positivas para parvalbúmina (PV) desempeñan un papel fundamental en la modulación de los procesos cognitivos. El sistema de orexina también participa en la regulación de la función cognitiva. Para proporcionar evidencia morfológica sobre la conexión neuronal entre las neuronas PV y orexina y su participación en la regulación de la función cognitiva en regiones cerebrales relacionadas con la función cognitiva, se empleó una tinción inmunohistoquímica de doble marcaje para PV y orexina para investigar las distribuciones superpuestas de la inmunorreactividad de PV y orexina en estas regiones cerebrales del ratón. Los somas de las neuronas PV y orexina se localizaron exclusivamente en el área hipotalámica lateral (LH), donde sus fibras también estaban estrechamente entrelazadas. En otras regiones, hubo diferentes grados de contacto y superposición entre las neuronas PV y las proyecciones de fibras de las neuronas orexínicas. Dentro del lóbulo frontal y el lóbulo temporal, se observó una superposición de densidad leve a moderada en la corteza orbitofrontal (OFC), la corteza prefrontal medial (mPFC), la corteza de asociación temporal (TeA) y la corteza perirrinal (PRh), mientras que la superposición fue relativamente escasa en la corteza entorrinal medial (MEnt). Se detectó una superposición de baja densidad en el putamen caudado (CPu). Dentro del prosencéfalo basal (BF), el núcleo accumbens (Acb), el núcleo septal medial (MS), el núcleo de la rama vertical de la banda diagonal (VDB), el núcleo de la rama horizontal de la banda diagonal (HDB), el pálido ventral (VP), la sustancia innominada (SI) y el núcleo preóptico magnocelular (MCPO) tuvieron diferentes grados de superposición. Se observaron distribuciones ligeramente superpuestas en el campo CA1 del hipocampo (CA1) y el giro dentado (DG) del hipocampo (HPC). Se encontró superposición de baja densidad en el núcleo amigdaloideo basolateral, parte anterior (BLA) y el núcleo amigdaloideo central (Ce) de la amígdala. Dentro del diencéfalo, se observaron diversos grados de contacto y superposición en el núcleo talámico reuniens (Re), el área hipotalámica anterior (AHA), el núcleo talámico mediodorsal (MD), el núcleo talámico paraventricular (PVT) y la zona incerta (ZI). Dentro del tronco encefálico, en la sustancia gris periacueductal (PAG) y el núcleo tegmental laterodorsal (LDTg), se detectó una gran cantidad de fibras de orexina entremezcladas y fibras finas ramificadas de PV, y también se observó superposición en el área tegmental ventral (VTA). En general, los somas de las neuronas PV y orexinas se colocalizaron sustancialmente en la LH. Las neuronas PV y las proyecciones fibrosas de las neuronas orexinas se conectaron y se entremezclaron en diversos grados en otras regiones cerebrales implicadas en la regulación de la función cognitiva. Estos hallazgos proporcionan evidencia morfológica que respalda la función correguladora de los sistemas PV y orexinas en la modulación de la función cognitiva.

PALABRAS CLAVE: Parvalbúmina Orexina; Función cognitiva; Memoria; Inmunohistoquímica.

REFERENCES

Averbeck, B. B. & Murray, E. A. Hypothalamic interactions with large-scale neural circuits underlying reinforcement learning and motivated behavior. *Trends Neurosci., 43(9)*:681-94, 2020.

Berger, C. C. & Ehrsson, H. H. The fusion of mental imagery and sensation in the temporal association cortex. *J. Neurosci., 34(41)*:13684-92, 2014.

Buzsáki, G. & Wang, X. J. Mechanisms of gamma oscillations. *Annu. Rev. Neurosci., 35*:203-25, 2012.

Bayard, S.; Croisier Langenier, M.; Cochen De Cock, V.; Scholz, S. & Dauvilliers, Y. Executive control of attention in narcolepsy. *PloS One, 7(4)*:e33525, 2012.

Carta, I.; Chen, C. H.; Schott, A. L.; Dorizan, S. & Khodakhah, K. Cerebellar modulation of the reward circuitry and social behavior. *Science, 363(6424)*:eaav0581, 2019.

Celio, M. R.; Babalian, A.; Ha, Q. H.; Eichenberger, S.; Clément, L.; Marti, C. & Saper, C. B. Efferent connections of the parvalbumin-positive (PV1) nucleus in the lateral hypothalamus of rodents. *J. Comp. Neurol., 521(14)*:3133-53, 2013.

Chen, Q.; de Lecea, L.; Hu, Z. & Gao, D. The hypocretin/orexin system: An increasingly important role in neuropsychiatry. *Med. Res. Rev., 35(1)*:152-97, 2015.

Chen, C. C.; Lu, J.; Yang, R.; Ding, J. B. & Zuo, Y. Selective activation of parvalbumininterneurons prevents stress-induced synapse loss and perceptual defects. *Mol. Psychiatry, 23(7)*:1614-25, 2018.

Cortese, S.; Konofal, E. & Lecendreux, M. Alertness and feeding behaviors in ADHD: does the hypocretin/orexin system play a role? *Med. Hypotheses., 71(5)*:770-5, 2008.

Dolan, R. J. Emotion, cognition, and behavior. *Science, 298(5596)*:1191-4, 2002.

Durairaja, A. & Fendt, M. Orexin deficiency modulates cognitive flexibility in a sex-dependent manner. *Genes Brain Behav., 20(3)*:e12707, 2021.

Deutch, A. Y. & Bubser, M. The orexins/hypocretins and schizophrenia. *Schizophr. Bull., 33(6)*:1277-83, 2007.

Fronczek, R.; van Geest, S.; Frölich, M.; Overeem, S.; Roelandse, F. W.; Lammers, G. J. & Swaab, D. F. Hypocretin (orexin) loss in Alzheimer's disease. *Neurobiol.Aging, 33(8)*:1642-50, 2012.

Franz, J.; Barheier, N.; Wilms, H.; Tulke, S.; Haas, C. A. & Häussler, U. Differential vulnerability of neuronal subpopulations of the subiculum in a mouse model for mesial temporal lobe epilepsy. *Front. Cell. Neurosci., 17*:1142507, 2023.

Gritti, I.; Manns, I. D.; Mainville, L. & Jones, B. E. Parvalbumin, calbindin, or calretinin in cortically projecting and GABAergic, cholinergic, or glutamatergic basal forebrain neurons of the rat. *J. Comp. Neurol., 458(1)*:11-31, 2003.

Hontanilla, B.; Parent, A.; de las Heras, S. & Giménez-Amaya, J. M. Distribution of calbindin D-28k and parvalbumin neurons and fibers in the rat basal ganglia. *Brain Res. Bull., 47(2)*:107-16, 1998.

Iaccarino, H. F.; Singer, A. C.; Martorell, A. J.; Rudenko, A.; Gao, F.; Gillingham, T. Z.; Mathys, H.; Seo, J.; Kritskiy, O.; Abdurrob, F.; *et al*. Gamma frequency entrainment attenuates amyloid load and modifies microglia. *Nature, 540(7632)*:230-5, 2016.

Liao, Y. X.; Zheng, Z. Y.; Cheng, X. F.; Wen, R. Y.; Xia, J. X.; Ren, S. C.; He, C. & Hu, Z. A. Regulatory role of lateral hypothalamus hypocretin neurons-medial entorhinal cortex neural circuit in spatial memory in mice. *J. Army Med. Univ., 45(09)*:927-35, 2023.

La Barbera, L.; Nobili, A.; Cauzzi, E.; Paoletti, I.; Federici, M.; Saba, L.; Giacomet, C.; Marino, R.; Krashia, P.; Melone, M.; *et al*. Upregulation of Ca2+-binding proteins contributes to VTA dopamine neuronsurvival in the early phases of Alzheimer's disease in Tg2576 mice. *Mol. Neurodegener., 17(1)*:76, 2022.

Lewis, E. M.; Spence, H. E.; Akella, N. & Buonanno, A. Pathway-specific contribution of parvalbumin interneuron NMDARs to synaptic currents and thalamocortical feedforward inhibition. *Mol. Psychiatry, 27(12)*:5124-34, 2022.

Murray, E. A. & Richmond, B. J. Role of perirhinal cortex in object perception, memory, and associations. *Curr. Opin. Neurobiol., 11(2)*:188-93, 2001.

McKenna, J. T.; Yang, C.; Franciosi, S.; Winston, S.; Abarr, K. K.; Rigby, M. S.; Yanagawa, Y.; McCarley, R. W. & Brown, R. E. Distribution and intrinsic membrane properties of basal forebrain GABAergic and parvalbumin neurons in the mouse. *J. Comp. Neurol., 521(6)*:1225-50, 2013.

Mészár, Z.; Girard, F.; Saper, C. B. & Celio, M. R. The lateral hypothalamic parvalbumin-immunoreactive (PV1) nucleus in rodents. *J. Comp. Neurol., 520(4)*:798-815, 2012.

Martínez, J. J.; Rahsepar, B. & White, J. A. Anatomical and electrophysiological clustering of superficial medial entorhinal cortex interneurons. *eNeuro, 4(5)*:ENEURO.0263-16.2017, 2017.

Nambu, T.; Sakurai, T.; Mizukami, K.; Hosoya, Y.; Yanagisawa, M. & Goto, K. Distribution of orexin neurons in the adult rat brain. *Brain Res., 827(1-2)*:243-60, 1999.

Nakazono, T.; Jun, H.; Blurton-Jones, M.; Green, K. N. & Igarashi, K. M. Gamma oscillations in the entorhinal-hippocampal circuit underlying memory and dementia. *Neurosci. Res., 129*:40-6, 2018.

Peyron, C.; Tighe, D. K.; van den Pol, A. N.; de Lecea, L.; Heller, H. C.; Sutcliffe, J. G. & Kilduff, T. S. Neurons containing hypocretin (orexin) project to multiple neuronal systems. *J. Neurosci., 18(23)*:9996-10015, 1998.

Pantazopoulos, H.; Lange, N.; Baldessarini, R. J. & Berretta, S. Parvalbumin neurons in the entorhinal cortex of subjects diagnosed with bipolar disorder or schizophrenia. *Biol. Psychiatry, 61(5)*:640-52, 2007.

Rudebeck, P. H. & Rich, E. L. Orbitofrontal cortex. *Curr. Biol., 28(18)*:R1083-R1088, 2018.

Roy, D. S.; Park, Y. G.; Kim, M. E.; Zhang, Y.; Ogawa, S. K.; DiNapoli, N.; Gu, X.; Cho, J. H.; Choi, H.; Kamentsky, L.; *et al*. Brain-wide mapping reveals that engrams for a single memory are distributed across multiple brain regions. *Nat. Commun., 13(1)*:1799, 2022.

Roque, P. S.; Thörn Perez, C.; Hooshmandi, M.; Wong, C.; Eslamizade, M. J.; Heshmati, S.; Brown, N.; Sharma, V.; Lister, K. C.; Goyon, V. M.; *et al*. Parvalbumin interneuron loss mediates repeated anesthesia-induced memory deficits in mice. *J. Clin. Invest., 133(2)*:e159344, 2023.

Roveta, F.; Marcinnò, A.; Cremascoli, R.; Priano, L.; Cattaldo, S.; Rubino, E.; Gallo, E.; Boschi, S.; Mauro, A. & Rainero, I. Increased orexin A concentrations in cerebrospinal fluid of patients with behavioural variant frontotemporal dementia. *Neurol. Sci., 43(1)*:313-17, 2022.

Sasaki, T.; Leutgeb, S. & Leutgeb, J. K. Spatial and memory circuits in the medial entorhinal cortex. *Curr. Opin. Neurobiol., 32*:16-23, 2015.

Stanojlovic, M.; Pallais Yllescas, J. P.; Jr, Vijayakumar, A. & Kotz, C. Early sociability and social memory impairment in the A53T mouse model of Parkinson's disease are ameliorated by chemogenetic modulation of orexin neuron activity. *Mol. Neurobiol., 56(12)*:8435-50, 2019.

Soares, V. P. M. N.; de Andrade, T. G. C. S.; Canteras, N. S.; Coimbra, N. C.; Wotjak, C. T. & Almada, R. C. Orexin 1 and 2 receptors in the prelimbic cortex modulate threat valuation. *Neuroscience, 468*:158-67, 2021.

Zhou, M.; Liu, Z.; Melin, M. D.; Ng, Y. H.; Xu, W. & Südhof, T. C. A central amygdala to zona incerta projection is required for acquisition and remote recall of conditioned fear memory. *Nat. Neurosci., 21(11)*:1515-9, 2018.

Corresponding author:
Maoyun Yuan
Department of Anatomy, Histology and Embryology
School of Basic Medical Sciences
Zhejiang Chinese Medical University
Hangzhou 310053
CHINA

E-mail: maoyun365@163.com

Corresponding author:
Jianping Zhang
Department of Anatomy, Histology and Embryology
School of Basic Medical College
Zhejiang Chinese Medical University
Hangzhou 310053
CHINA

E-mail: zjpzzq@163.com